A Machine Vision for Automated Headlamp Lens Inspection

Chapter · August 2010

DOI: 10.5772/10134 · Source: InTech

4 authors, including:

Silvia Satorres
University of Jaén
44 PUBLICATIONS **519** CITATIONS
SEE PROFILE

J. Gamez Garcia
University of Jaén
109 PUBLICATIONS **1,224** CITATIONS
SEE PROFILE

Alejandro Sánchez
University of Jaén
18 PUBLICATIONS **70** CITATIONS
SEE PROFILE

4

A Machine Vision System for Automated Headlamp Lens Inspection

S. Satorres Martínez, J. Gómez Ortega,
J. Gámez García and A. Sánchez García
Electronic Engineering and Automation Department. University of Jaén
Jaén, Spain

1. Introduction

Headlamps on vehicles are primarily responsable for illuminating the traffic space during periods of low visibility, such as night or precipitation. In addition, headlamps are also considered as a cosmetic part, playing an important role in the car styling. Because of this, carmakers request a great precision for surface defect detection in all the headlamp components.

One of these components is the cover lens (Fig. 1). This part used to be made of glass but polycarbonate lenses have become today's standard. In comparison to glass, plastic lenses have the advantages of higher resistance to impact, lower weight, small manufacture tolerances and much greater freedom of design thanks to the possibility of undercuts [Wördenweber et al. (2007)]. But for scratch resistance, policarbonate lenses must be coated. Failures during the manufacturing and coating process lead to different kind of defects known as *aesthetic defects*. Although this kind of defects do not entail any functional disadvantage, may be considered as aesthetically displeasing.

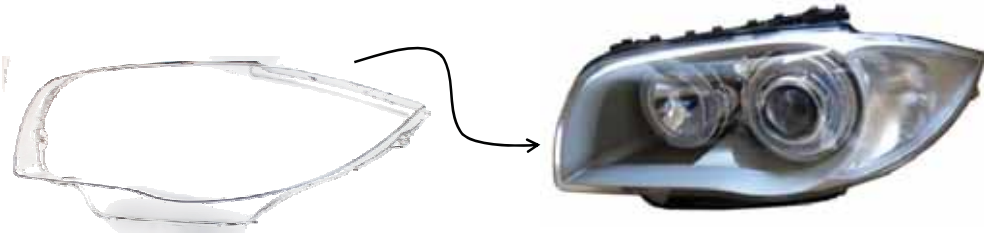

Fig. 1. The Serie 1 BMW headlamp and its cover lens.

Nowadays, the quality control of the lenses is made by manual means. The results of this process depend on *human factors* as subjectivity and visual tiring, that may lead to a dissatisfactory quality control. For this reason, a fully automated inspection system is highly desirable.

This chapter presents a machine vision system capable of revealing, detecting and characterizing *aesthetic defects* on headlamp lenses. Due to its geometry and dimensions, this part requires multiple vision sensor poses to completely observe it and, our proposal,

performs an automatic selection of these poses. For this task, a sensor planning system that computes the number and sensor locations has been developed. This system includes useful information provided by the human inspector, as the maximum defect size that should be located in every lens area, to fix better the sensor poses. In order to code the expert information for including it in the sensor planning system, a fuzzy rule based system is also developed. To compute the number and distribution of vision sensors, the planning system applies a genetic algorithm.
Furthermore, as some kind of defects and the lens have the same optical properties, special lighting conditions are required to enhance defects and to simplify the subsequent processing algorithms. To solve this problem, we also introduce in this chapter the special lighting conditions required, presenting the lighting techniques capable of revealing defects, with different optical properties, on transparent parts. Once the acquisition stage is finished, the images should be processed to extract suitable information. So, the computer vision algorithms involved in delivering this kind of information should be defined.
The chapter is organized as follows. In the next section, the task that the machine vision system has to accomplish is described; also a former work that offers a global solution to the automated inspection of lenses. Section 3 presents the proposed machine vision system describing, in detail, all its components. Finally, the machine vision is experimentally tested using a commercial lens model and the results are offered in Section 4, whereas Section 5 outlines the conclusions of this work.

2. Problem description: the headlamp lens inspection

To date, the quality control of headlamp lenses is visually made by an expert operator, or simply, by an inspector, that checks the absence of aesthetic defects on the lens surface. He also decides if it has to be rejected or packaged for further processing. The aesthetic defect sizes may vary from tenths of millimeter to centimeters and, according to their shape, can be divided into the following groups (Fig. 2):

- punctual defects (bubbles, blisters and black points);
- lineal defects (threads, scratches);
- surface defects (excesses of varnish, orange skin).

Fig. 2. Aesthetic defects. From left to right: punctual and opaque defect (a black point), punctual and transparent defect (a blister), lineal defect (a scratch) and surface defect (excesses of varnish).

Moreover, to meet the customer requirements, and also to establish a standard in this manual process, the inspector must follow the *inspection guideline*. This guideline is a document which presents the acceptance and rejection criterions for the lens. The time

invested to inspect the lens and the visual path that the inspector must follow during the inspection are also described in this document. Normally, a sketch of the lens divided into colored areas is presented to define the rejection criterions. Every color indicates different inspection requirements, so the defect dimension that has to be located in each lens area differs from one to another (Fig. 3).

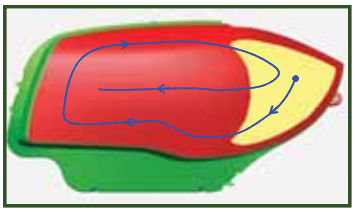

Defect geometry	Red	Yellow	Green
Punctual mm	0.7	1	1.5
Surface mm	Not visible P/V	6	10
Linear mm	1	2	5

Fig. 3. Information presented in the inspection guideline.

Due to the complexity of the defects to be detected: small size, different optical properties—transparent, opaque—and geometries, it is desirable to offer a robust solution capable of automating the lens inspection process. In this respect, machine vision provides innovative solutions for automatic surface inspection systems [Malamas et al. (2003)] and this technology had been used in the first attempt to automate the lens inspection. The development was a machine vision prototype known as VIGILE (Visual Intelligent Glass Imperfections Looking Equipment)[Automation & Robotics (2001)]. It was supposed that by successive scanning of the surface of the lens, that was laid down on a specific automatically adaptable carrier, VIGILE detected different types of defects using three stations of inspection. This machine vision system could be adapted to inspect four model of lenses. Finally, this prototype was not commercialized because it did not fit to the lens manufacturers expectations.

Our proposal presents substancial differences respect to the VIGILE system. Firstly, for the image acquisition the lens surface is not scanned; instead of this, a set of suitable sensor poses is computed through a sensor planning system. Secondly, defects with different optical properties are not identified in several stations of inspection. In our machine vision system, only one lighting device with flexibility for selecting different lighting techniques is utilized. As regards the image processing, the information about the computer vision algorithms included in the VIGILE was not available. In our case, and thanks to the lighting system, the images are processed utilizing algorithms with a very low computational burden, allowing the real time inspection.

3. The machine vision system

To accomplish the automated inspection of lenses, a machine vision system has been developed and it is presented in figure 4. This system consists of the following components:

- an anthropomorphic 6-DOF Stäubli RX60 industrial manipulator and a CS8 controller;
- a firewire monochrome vision sensor GUPPY F-080B;
- a TFT monitor as lighting system;
- a host PC to mainly compute the sensor poses, to control the lighting system and to process the images.

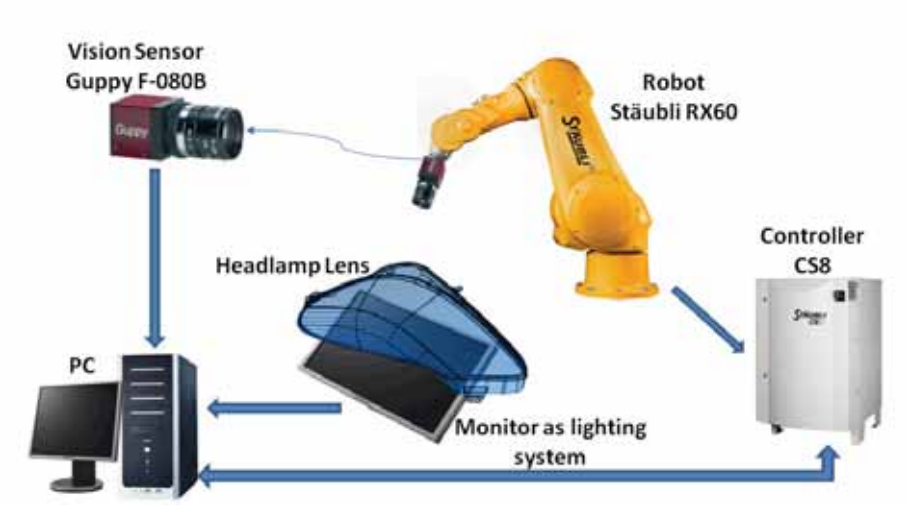

Fig. 4. The machine vision system.

The attention is first focused in the image acquisition. The monochrome vision sensor is mounted, as end-effector, on the industrial manipulator. This enables flexibility and accuracy in the vision sensor poses being easily adaptable to different lens models. The vision sensor poses are computed off-line using a host PC. Also, the computer vision algorithms are executed in it.

As regards the lighting system, the machine vision includes a TFT monitor. This device enables flexibility for selecting different lighting solutions, specially adapted to enhance all the types of aesthetic defects [Satorres Martínez et al. (2009c)]. The next subsections are dedicated to introduce the steps that had been carried out to finally automate the lens inspection process. They are:

- planning the sensor poses;
- selecting the lighting system;
- the image processing.

3.1 Planning the sensor poses

In occasions, one single viewpoint is not enough to sample the whole surface of a part. This is the case of a headlamp lens, that due to its geometry, size and the dimension of defects that have to be located in its surface requires multiple sensor poses to observe it.

The problem of automating the sensor vision poses in order to select suitable viewpoints for the object inspection is know as sensor planning or sensor placement [Sheng, Xi, Tan, Song&Chen (2003)]. Several researchers have proposed sensor planning approaches that fall into two main categories [Tarabanis, Allen & Tsai (1995)]: *generate-and-test* and *synthesis*. The *generate-and-test* approach [Kakikura (1990)], [Yi et al. (1990)] simplifies the sensor planning into a search problem in a restricted solution space. Although it is straightforward and easy to implement, the computational cost is very high due to the large number of candidate viewpoints.

Contrary to the *generate-and-test*, the *synthesis* approach [Cowan & Kovesi (1988)], [Tarabanis, Tsai & Allen (1995)] requires a deeper understanding of the relationships

between the parameters to be planned—sensor poses and optical parameters—and the goals to be achieved. Task constraints are characterized analytically and the sensor parameter values, that satisfy these constraints, are directly determined from the analytical relationships. However, this approach has two main drawbacks. Firstly, constraint equations in high dimensional space that are not easy to solve; and secondly, it is very difficult to mathematically express the exact solution regions to these equations. Other ongoing work combines the previous methodologies for solving the problem [Sheng, Xi, Song & Chen (2003)], or study it under a multi-objective framework [Dunn (2005)].
In the proposed machine vision system a sensor planning system, that automatically generates a set of vision sensor poses for inspecting the lens, has been developed. This system is deeply described in [Satorres Martínez et al. (2009d)] but its main components are stated below.

3.1.1 The sensor planning system

The Sensor Planning System (SPS) (Fig. 5) requires several inputs to achieve its goal. First, a detailed specification about the environment (e.g., the object under observation, the available sensors, other useful information for the inspection task) should be provided. Then, the SPS automatically determines the vision sensor parameter values (e.g., number of sensors and their poses) to take images from the whole headlamp lens. In order to determine an optimal set of vision sensor poses the SPS uses a genetic algorithm. Therefore, the system inputs and the corresponding output are the following:

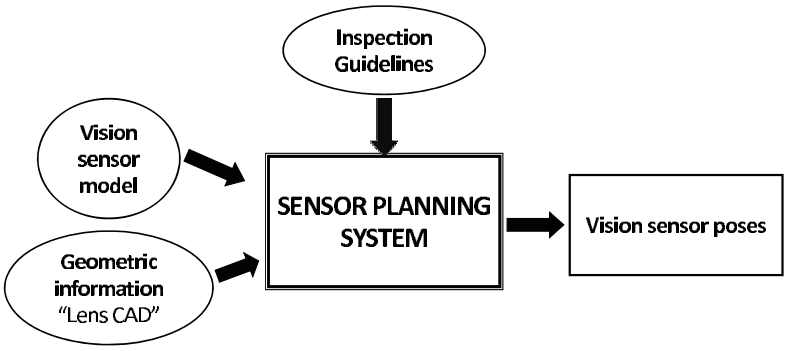

Fig. 5. The sensor planning system.

1. System inputs.
   The a priori known information is taken into account in the viewpoint computation:
   a. geometric and physical information of the headlamp lens that is extracted from its CAD model;
   b. a vision sensor model that approximates its geometrical properties. The model adopted is the pin-hole lens model. This model assumes that light rays travel in straight lines and all the rays entering the vision sensor system pass through a single point [Forsyth & Ponce (2003)];
   c. the *inspection guideline* that provides the acceptance and rejection criterions for lenses. As this document is defined by experts in lens inspection to model this knowledge, for including it in the SPS, a Fuzzy Rule-Based System (FRBS) has been developed. This FRBS was initially presented in [Satorres Martínez et al. (2009a)].

2. System output.
   For each viewpoint the SPS computes four positional parameters (Fig. 6):
   a. three degrees of freedom of viewpoint's position. These are the vision sensor Cartesian coordinates in the world coordinate system;
   b. one degree of freedom of viewpoint's orientation (θ_{Z_c}). This angle corresponds to the vision sensor rotation around its optical axis. The other degrees of freedom in the viewpoint's orientation, θ_{X_c} and θ_{Y_c} angles, are not considered, since the optical axis of every point of view is set to look inward to the nearer lens area.

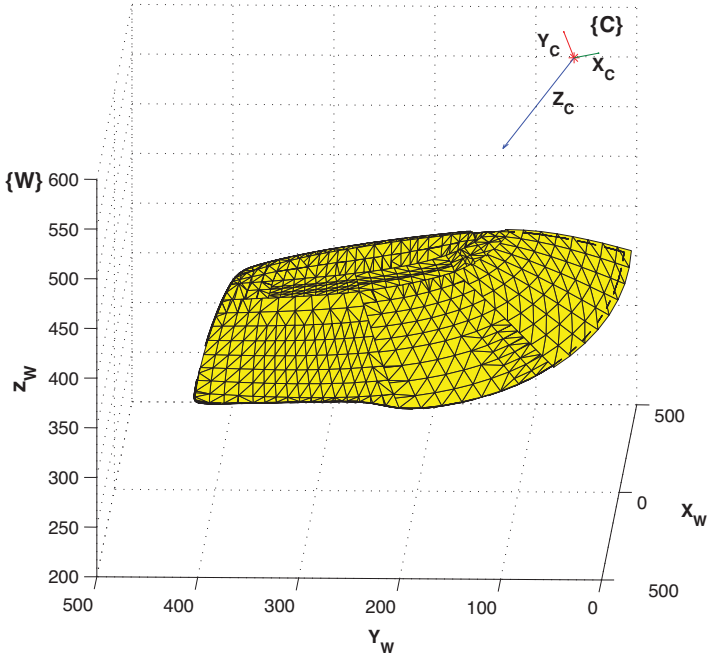

Fig. 6. A vision sensor pose and the lens CAD model.

Moreover, an admisible viewpoint should satisfy the following constraints that are checked in the following order:

a. *visibility*: this constraint ensures that there is no occlusion between the viewpoint and the lens surface to be inspected;
b. *field of view*: vision sensors have limited field of view by the size of the sensor area and the focal length of the lens. The homogeneous transformation matrix is used to compute the surface points that will be projected inside the sensor area. This mathematical modeling gives a direct relation between the camera and world coordinate systems. So, the image coordinates x and y of a point in the world coordinate system ${}^{W}P$ are obtained from:

$$x = \frac{{}^{c}P_1}{{}^{c}P_4} = \frac{a_{11} \cdot X + a_{12} \cdot Y + a_{13} \cdot Z + a_{14}}{a_{41} \cdot X + a_{42} \cdot Y + a_{43} \cdot Z + a_{44}} \tag{1}$$

$$y = \frac{{}^{c}P_2}{{}^{c}P_4} = \frac{a_{21} \cdot X + a_{22} \cdot Y + a_{23} \cdot Z + a_{24}}{a_{41} \cdot X + a_{42} \cdot Y + a_{43} \cdot Z + a_{44}} \tag{2}$$

where a_{ij} are the elements of the homogeneous transform matrix ${}^{c}_{w}T$ that relates the vision sensor and the world coordinate systems through a rotation, translation and perspective transform [Satorres Martínez et al. (2009d)]. A point in the world coordinate system ${}^{w}P$ can be referenced in the vision sensor coordinate system ${}^{c}P$ as:

$$\begin{bmatrix} {}^{c}P \\ \cdots \\ 1 \end{bmatrix} = {}^{c}_{w}T \cdot \begin{bmatrix} {}^{w}P \\ \cdots \\ 1 \end{bmatrix} \tag{3}$$

c. *viewing angle*: implies that the curvature of the field of view can be chosen by selecting a limit between the viewing direction and the normal of the surface points;
d. *resolution*: ensures that the smaller size of defect accepted in every lens area with length l is imaged to at least p pixels on the image plane. Considering the lens model (Fig. 7), the following can be formulated:

$$x_s = \frac{h}{f} \cdot p \cdot x_c \leq l \tag{4}$$

where x_s is the scene feature size, h is the distance from the camera lens to the surface to be inspected, f is the focal length and x_c is the pixel size.

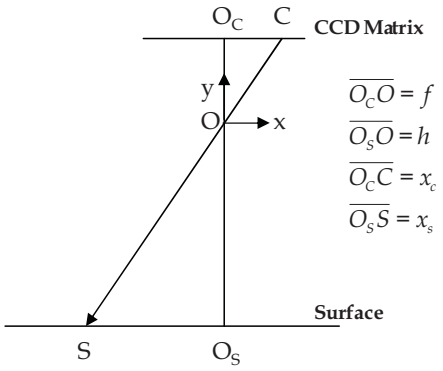

Fig. 7. Resolution constraint.

3.1.2 Optimal sensor placement

With respect to the genetic algorithm, developed for the optimal vision sensor placement, two main aspects are worthy of mention:

- representation of candidate solutions to the problem in a ”genetic” form (*chromosome representation*);
- establishment of a *fitness function* that rates each solution in the population.

The genetic operators to produce new individuals from the exiting ones are widely used in evolutionary computing [Eiben (2003)] and also are deeply described in [Satorres Mart´ınez (2010)].

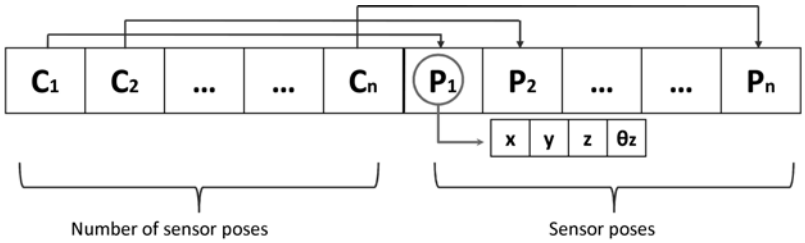

Fig. 8. Chromosome structure.

1. Chromosome representation.
   The chromosome contains two different type of genes (Fig. 8): control genes and parametric genes [Chen & Li (2002)]. Parametric genes ($P_i = (x,y,z,\theta_z)$) mean the sensor poses with $x,y,z \in \mathbb{R}$, $\theta_z \in [-\pi,\pi]$, and control genes (C_i) are a binary variable meaning the number of viewpoints. The activation of the parametric genes is governed by the value of the control genes.
   When "1" is assigned to a control gene, the associated parametric gene to that particular active control gene is activated. The parametric genes are inactive when the corresponding control genes are "0".
   To determine the chromosome length, the maximum number of viewpoints must be estimated through [Chen & Li (2004)]:

$$N = \frac{2 \cdot S_{lens}}{S_{view}} \tag{5}$$

   where S_{lens} is the lens surface area size and S_{view} is a single view size. So, the length of a chromosome is expressed as: $N + k \cdot N$, where N is the maximum number of viewpoints and k is the number of parameters planned for each point of view. With this chromosome representation, all individuals in the population have the same size, but the number of active viewpoints may be variable.
2. Fitness function.
   Each individual of the population is evaluated by a fitness function (Eq. (6)), that is given as a weighted sum of two contradictories objectives, each of which characterizes the quality of the solution with respect to an associated requirement. Thus, the fitness function is written as

$$F = w_1 \cdot OBJ_1 + w_2 \cdot (1 - OBJ_2) \tag{6}$$

   where w_i are the weighting coefficients and OBJ_i are the objectives that have to be satisfied being summarized as follows:
   a. **OBJECTIVE 1** (OBJ_1):
      Minimizing the number of viewpoints (C_i):

$$OBJ_1 = \min \frac{\sum_{i=1}^{n} C_i}{n_C} \tag{7}$$

      where the number of occurrences of "1" in the control genes is equivalent to the number of viewpoints for each chromosome, and n_C is the number of control genes.

b. **OBJECTIVE 2** (OBJ_2):
Maximizing the accuracy of the vision inspection, that is, how the resolution of every camera pose fits to the resolution required to inspect its scanned lens area.
To evaluate this objective a two-dimensional binary array, known as the *quality matrix* (q_m), is created by:

$$q_m(i,j) = \begin{cases} 1 & \text{if } s_j \text{ fulfill the constraints for } v_i \\ 0 & \text{otherwise} \end{cases} \quad (8)$$

q_m will be an array of $r \times c$ dimensions, where r is the number of viewpoints and c is the number of CAD finite elements. If $q_m(i, j) = 1$ the surface point s_j is viewable from the viewpoint v_i and also fulfills the aforementioned constraints.
Nevertheless, a column of 0's in the quality matrix means that there is some surface point that cannot be seen by the available sensor poses and therefore it is not possible to create a plan that can view the entirely of the lens. Conversely, if there are not nonzero-columns, a plan to view the whole lens exists.

3.2 The lighting system

In computer vision applications, the provision of a correct and high-quality illumination is absolutely decisive [Telljohann (2008)]. Hence, the light needs to be provided in a control manner to accentuate the desired features of the surface avoiding disturbances which could alter the quality of the acquired image. So, an inadequate lighting system selection involves the development of complex computer vision algorithms to extract information from the images, or even imply an unfeasible vision task [Jahr (2008)]. Finding the best setup is usually a result of experiments with commercial lighting systems. Next subsection shows the main experiences obtained evaluating several lighting techniques to enhance aesthetic defects on the lens surface.

3.2.1 Lighting techniques

There is a rich variety of lighting techniques that may be used in machine vision. From the available commercial lighting systems, the most recommended for this application are the back-light and the diffuse dark field systems and both of them have been studied.
The diffuse back-light achieves non-directional uniform illumination resulting in a bright image, whereby surface features appear in gray levels. This technique is normally used for viewing the silhouette of opaque objects and for inspecting transparent ones. But this light is suitable when the contrast between different surface qualities is high so, in the lens, only not-transparent surface defects are revealed (Fig. 9).
Concerning the dark field illumination, the angle of the incident light rays to the surface normal vector is very large. This results in a dark appearance of the surface, but salient features, such as scratches, appear bright in the image. Hence, this type of illumination is used to detect small particles in flat parts. In addition, applied this lighting system to the less curvature areas in the lens only revealed surface dirt as dust (Fig. 10).
Another lighting technique, that it is utilized for inspecting reflective surfaces is the structured lighting [Seulin et al. (2001)] and [Aluze et al. (2002)]. Adapting this technique for inspecting the lens surface, the transparent aesthetic defects can be enhanced. So, the lighting principle in which it is based this kind of structured back-light system is the following (Fig. 11): the orientation of a surface imperfection is different from the flawless

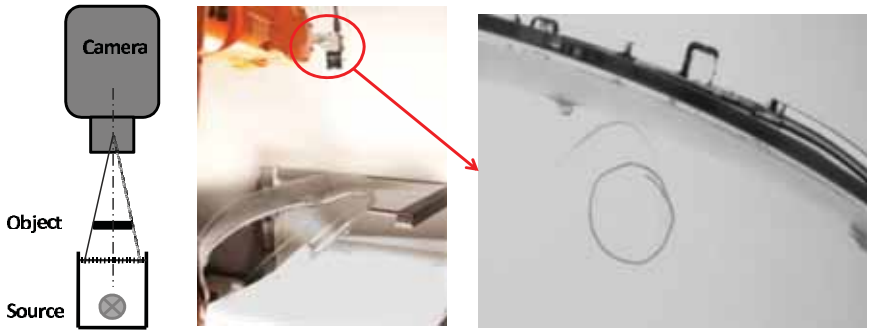

Fig. 9. Diffuse back-light. From left to right: principle of lighting; robotic platform with back-light illumination; the image acquisition.

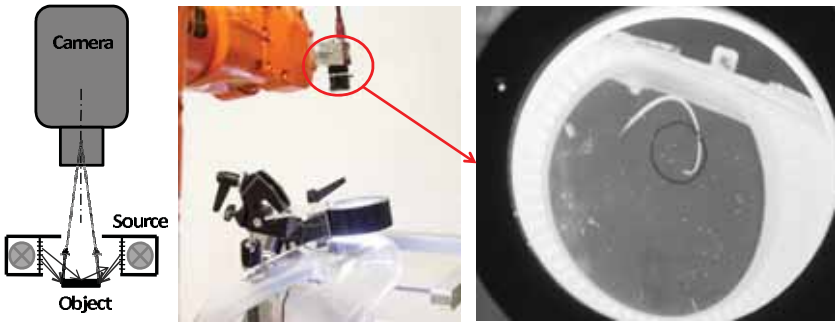

Fig. 10. Diffuse darkfield. From left to right: principle of lighting; robotic platform with darkfield illumination; the image acquisition.

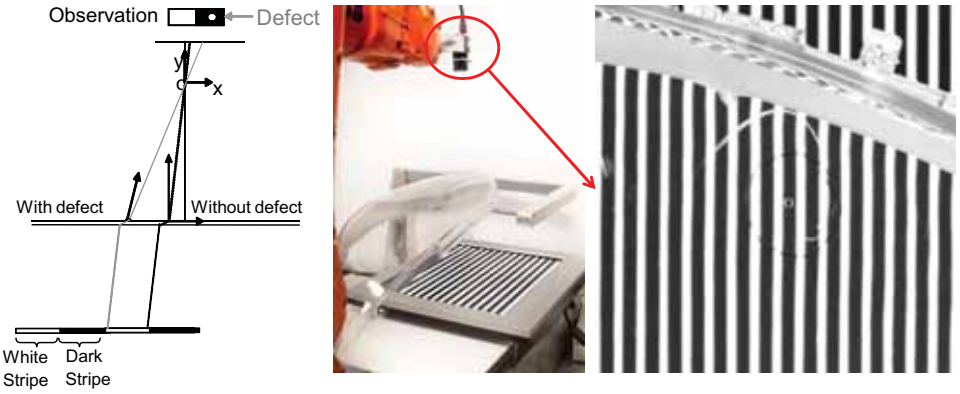

Fig. 11. Structured lighting. From left to right: principle of lighting; robotic platform with structured lighting; the image acquisition.

ones, so incident ray lights are not scattered in the same direction [Coulot et al. (1997)]. Therefore, a defect, because of its orientation, appears in the capture image as a set of luminous pixels among a dark zone. It is interesting to point out that the imperfections are properly revealed when they are next to the light transitions. So, to ensure the defect detection in the whole lens surface, the light stripes have to scan all over the sensor field of view.
As it can be seen, two lighting techniques should be applied for enhancing aesthetic defects: the backlight (for opaque defects) and the structured back-light (for transparent ones). This flexibility is achieved with our lighting system: a TFT monitor.

3.2.2 The TFT monitor as lighting system

In the proposed machine vision system a TFT monitor has been adopted as lighting. Previous work have also used this kind of illuminator but for different purposes as surface measurement [Guo (2007)], surface reconstruction [Kutulakos (2008)] or subsurface crack detection [Chan (2008)]. In our case, the TFT monitor has been included in the vision system mainly for:

- flexibility: one device provides two lighting techniques;
- easy to generate and to modify: the light pattern—the white and black stripes—can be adapted to reveal defects with different sizes;
- accurate pattern movement: from every sensor pose several images with different stripe displacement should be acquired. With this lighting system the stripe movement is done by software so, the movement is not subjected to mechanical imprecisions.

In addition, the set of images acquired from every sensor pose should be processed using computer vision algorithms with a very low computational burden. This issue is also achieved processing an image composed from this sequence. In previous work, this image has been denoted as *aspect image* [Satorres Martínez et al. (2009b)] and a determined procedure has to be applied for obtaining it.

3.3 The image processing

The whole inspection process, starting in the image acquisition and finishing in the defect characterization, is exposed in the flowchart presented in figure 12. As shown, the acquisitions are synchronized with the stripe movements and when the white stripe covers the dark stripe width completely, the image sequence is finished. From this set of images, the *aspect image* is obtained and all the subsequent processing algorithms are applied on predefined regions of this composition. Once the set of pixels, labeled as possible defects, are extracted from the background, the decision of rejecting the lens is based on the measurement parameters—such as the defect size—considered in the manual inspection process and presented in the *inspection guidelines*.

3.3.1 The aspect image

Let consider a one-dimensional representation of the lighting system being a square waveform ($P(x)$) and the white stripe T_B has to scan the whole period of the wave (T)(Fig.13), where:

- Δ: displacement between stripes in two consecutive images.
- α: duty cycle.

To obtain an image where the background appears with medium gray level and defects as high gray level, the mean image of the N waveform sequence has to be computed as:

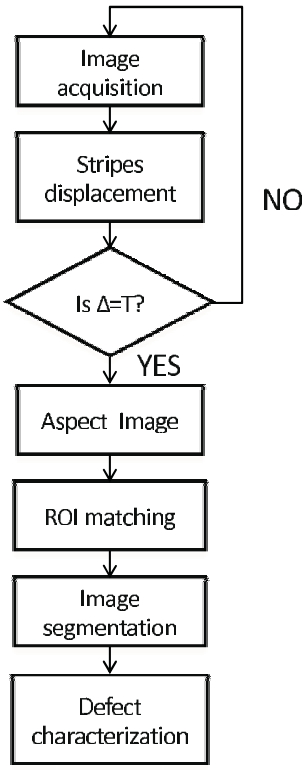

Fig. 12. The image processing flowchart.

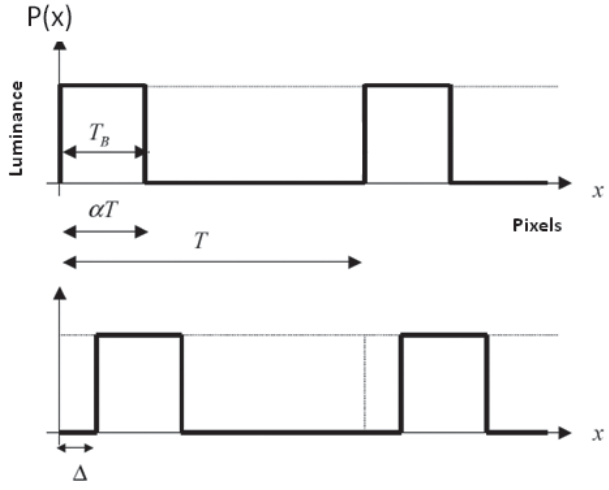

Fig. 13. Lighting system geometric information

$$M(x) = \frac{1}{N} \cdot \sum_{n=0}^{N-1} P(x - n \cdot \Delta) \quad n \in \mathbb{N} \tag{9}$$

$$\Delta = \frac{\alpha \cdot T}{s} \quad s \in \mathbb{N} \quad 1 \le s \le \alpha \cdot T \tag{10}$$

where $M(x)$ is called *aspect image* and the homogeneity of the background is critical in the defect segmentation. So, the imaging conditions have to be chosen in order to provide *aspect images* with a background the more homogeneous as possible.

3.3.2 Defect segmentation

Image segmentation can generally be described as separating images into various regions or objects in which the pixels have similar characteristics [Russ (2007)]. This is an important task, in that the image interpretation relies strongly on its results. In our case of study, and previous to the segmentation step, the image regions, where the processing algorithms have to be applied, should be defined.

In computer vision applications, these regions are known as Regions Of Interest (ROI) and if they are not defined, false detection could perturb the defect characterization. This definition is particularly important on the lens edges or on the lens surfaces that are not completely smooth. As we perform the inspection in a robotic platform, repetitive vision sensor positioning is achieved. So, for every sensor pose, a binary mask is defined where pixels labeled with "1" are later processed.

Because of the well contrasted *aspect image* and the homogeneity of its background, no preprocessing algorithms are required. Dealing with this sort of image, the automatic thresholding methods are widely used for segmentation [Ng (2006)]. The basic idea of these methods is, based on the gray-level distribution derived from the image histogram, to select a threshold value for separating objects of interest from the background.

The aspect image histogram presents an unimodal distribution because most of the pixels are included in the background and have a similar medium gray-level. Only aesthetic defects present a high gray-level but constitute a disproportionately small number of pixels of the whole image. There is a thresholding algorithm suitable for segmenting images that present an unimodal histogram distribution. This is the Rosin algorithm [Rosin (2001)] that estimates an automatic threshold by computing the following expression:

$$U_{opt} = arg\ max \left[\frac{\left| (x_f - x_s) \cdot (y_s - h(g)) - (x_s - g) \cdot (y_f - y_s) \right|}{\sqrt{(x_f - x_s)^2 + (y_f - y_s)^2}} \right] \tag{11}$$

where (x_s, y_s) correspond to the dominant peak of the histogram and (x_f, y_f) are relative to the secondary population that may not produce a discernible peak but it is well separated from the large peak. The values g and $h(g)$ are the gray-level and the number of pixels with gray-level g, respectively.

3.3.3 Defect characterization

Once the defects are extracted from the flawless area, they have to be measured to determine if the lens could be accepted or, however, has to be rejected. The measurement parameters and the acceptance thresholds are extracted from the *inspection guidelines* and

they correspond to the ones used in the manual inspection process. These parameters are normally the following:

- The size in mm^2 of the defect. This measure is to characterize punctual defects.
- The longitude in mm of the major axis of the defect. Useful for characterizing lineal defects.
- The number of defects.

Because the vision sensor is posed normal to the lens surface, the number of active pixels "1s" corresponding to a defect, is a linear function of the defect occupancy surface. Hence, no perspective correction is required to measure the defect that have been extracted in the previous step.

4. Results

On this section different types of results, that have been obtained during the validation of the machine vision system, are presented. Firstly, a set of sensor poses computed with the sensor configurations defined in the table 1 is obtained with our planning system. The planning results were subsequently utilized to acquire the images from the whole lens surface. Later, the effectiveness of the lighting system for enhancing aesthetic defects is demonstrated using defective lenses that have been rejected in the manual inspection process. The lighting system configuration is also presented in table 1. Finally, related to the computer vision algorithms, their performances are assessed by processing a serie of aspect images acquired using a commercial model of lens. For this lens model, the minimum defect size that has to be detected is a punctual defect of $1mm$ of diameter.

Vision Sensor	
Parameters	**Values**
Resolution	1034×778
Pixel size	$0.00465mm$
Focal length	$25mm$
Spatial resolution	$0.1mm/pixel$
Lighting System	
Parameters	**Values**
T_B	6 *pixels*
T	18 *pixels*
Δ	1 *pixel*

Table 1. Sensor and lighting system configuration

4.1 The sensor planning system

The set of sensor poses is presented in the figure 14. This set has been obtained adjusting higher the weighting coefficient (w_2) in the fitness function. In this case, the second objective has been prioritized so, from all the sensor poses, the spatial resolution should be enough to guarantee the aspect defect detection. As can be seen, with 22 sensor poses the whole lens surface is inspected and in all the sensor poses the spatial resolution is enough to ensure the defect detection. The table 2 shows the two extreme sensor poses with their distances to the

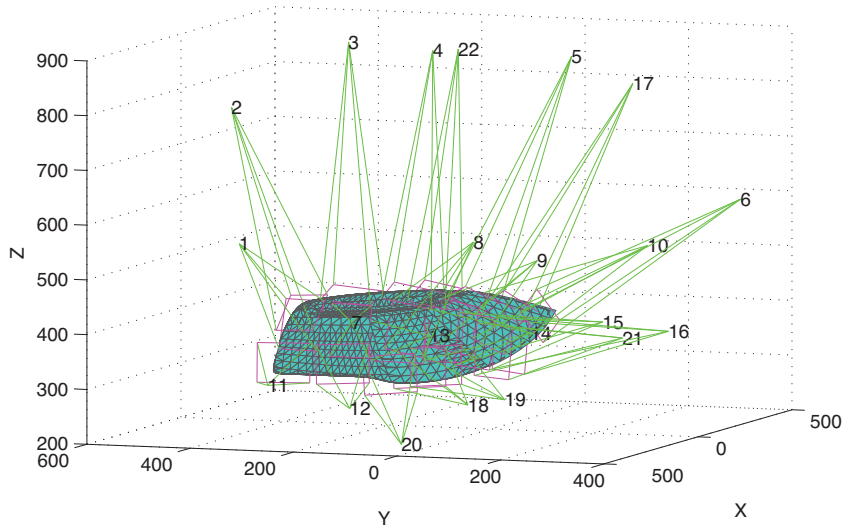

Fig. 14. The planning results.

lens surface and the defect size that could be detected from them. In fact, in the sensor pose with a greater distance to the lens surface the defect size that could be detected is 0.96 *mm* which is lower than the defect size that has to be located for this lens model.

Sensor pose	**Distance from the vision sensor to the lens surface** (*mm*)	**Defect size** (*mm*)
6	483	0.8
20	520	0.96

Table 2. Sensor poses and their distances to the lens surface.

4.2 Enhancing aesthetic defects

A TFT monitor as lighting system has been utilized in the machine vision system for enhancing the aspect defects. This device offers two lighting techniques that could be adapted to reveal opaque and transparent defects. Figure 15 shows two types of punctual defects and how they are enhanced with the our lighting system. For the opaque punctual defect (Fig. 15a) the TFT monitor projects an homogeneous background performing as a conventional back-lighting system. However, the transparent defects are only enhanced projecting a stripe pattern (Fig. 15b). Later, and thanks to the image composition this type of defects are clearly contrasted from the lens surface (Fig. 15c).

4.3 Characterizing aesthetic defects

Once the aspect image is achieved it has to be processed for deciding if the lens has to be rejected or accepted. The figures 16 and 17 show the aspect image segmentation and how the regions of pixels extracted in each figure have been labeled. In both cases, if the number of pixels in a region is higher than 50, the corresponding region, is considered as an aesthetic defect. According to the sensor configuration and the distances from the vision sensor to the lens surface, this region size coincides with a defect length or diameter of 1*mm*. In this

respect, all the segmented regions in figure 16b have a dimension lower than 50 pixels and because of this are labeled as *OK*. On contrary, one of the segmented regions in the figure 17b has a dimension higher than 50 pixels. For this reason, an aesthetic defect has been located in this aspect image labeling the region as *KO*.

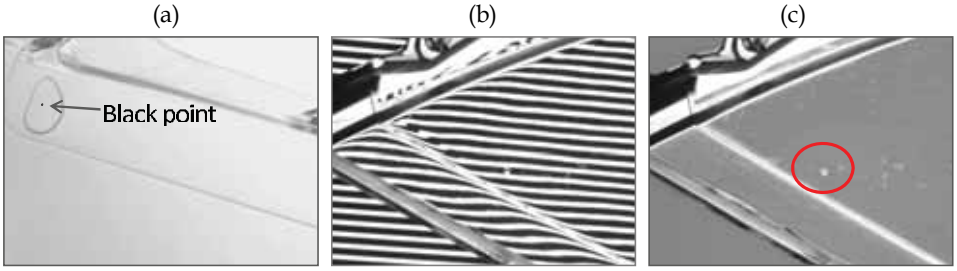

Fig. 15. Enhancing aesthetic defects: (a) Opaque punctual defect; (b) Transparent punctual defect with the stripe pattern; (c) Transparent punctual defect in the aspect image.

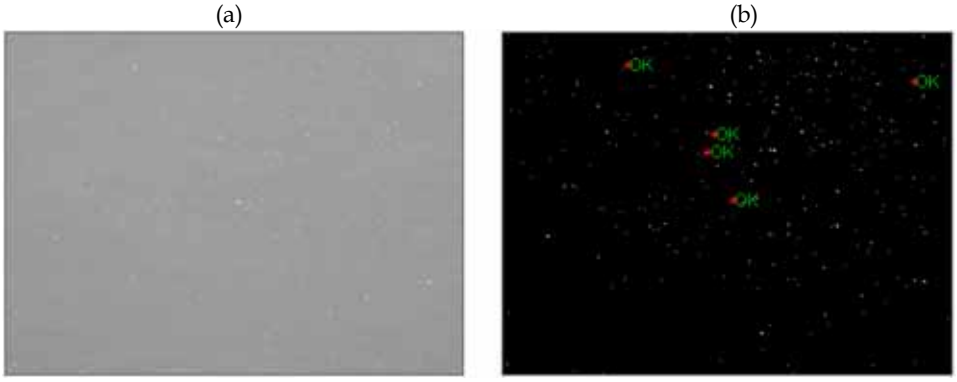

Fig. 16. Processing results: (a) Aspect image without aesthetic defects; (b) Aspect image segmentation and characterization.

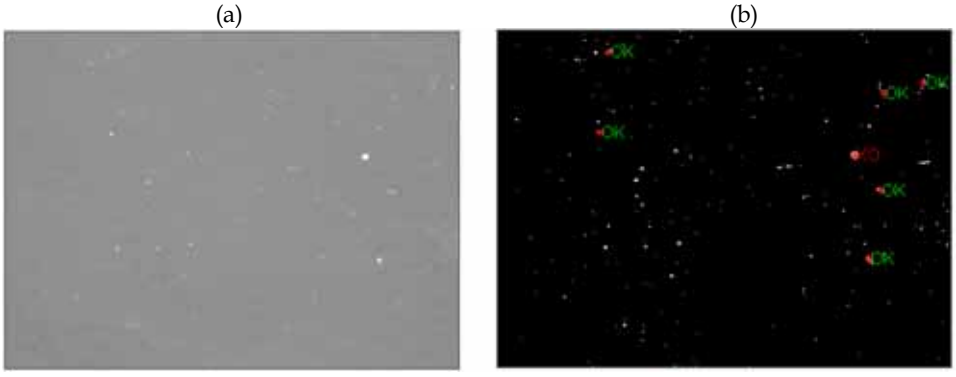

Fig. 17. Processing results: (a) Aspect image with a transparent punctual defect; (b) Aspect image segmentation and characterization.

5. Conclusions

This chapter is dedicated to develop a machine vision system for the automated inspection of headlamp lenses. The quality control of this part is a complex task that nowadays is made by manual means. Its complexity is due to the fact that, the proportion between the aesthetic defect size and the lens dimension is high. Moreover, some defects may be transparent, as the lens surface, and revealing them require a particular lighting conditions.

Both issues are taken into account in the proposed machine vision system. Firstly, to observe the whole lens surface several vision sensor poses should be defined. In this work, the sensor poses are computed automatically through a sensor planning system. In some lens models, the aesthetic defect size is variable depending on the lens zone where it was located. This information is utilized in the planning system allowing to fit better the number of sensor poses. It is worth noticing that the machine vision system could be easily adapted to inspect different lens models.

Secondly, the lighting system enables the detection of transparent and opaque defects using different lighting techniques. It is possible using a TFT monitor and projecting two light patterns: an homogeneous white background or white and black stripes. The first pattern enhances the opaque defects and the second reveals the transparent ones. On the other hand, the image processing has been carefully studied. The computer vision algorithms are applied to an image composition named as *aspect image*. In this image, the aesthetic defects appear well contrasted and the image background is totally homogeneous. So, the defect segmentation is fast to compute using a global thresholding algorithm. Finally, with our system, a set of a commercial model of headlamp lenses have been analyzed demonstrating that the automated inspection of this part is a feasible task.

6. References

Aluze, D., Merienne, F., Dumont, C. & Gorria, P. (2002). Vision system for defect imaging, detection, and characterization on a specular surface of a 3d object, *Image and Vision Computing* 20: 569–580.

Automation & Robotics (2001). http://www.ar.be/index.htm.

Chan, F. (2008). Reflective fringe pattern technique for subsurface crack detection, *NDTE International* 41: 602–610.

Chen, S. & Li, Y. (2002). A method of automatic sensor placement for robot vision in inspection tasks, *Proc. IEEE Int. Conf. on Robotics and Automation* 3: 2545–2550.

Chen, S. & Li, Y. (2004). Automatic sensor placement for model-based robot vision, *IEEE Transaction on Systems, Man and Cybernetics - Part B: Cybernetics* 34(1): 393–408.

Coulot, C., Kohler-hemmerlin, S., Dumont, C., Aluze, D. & Lamalle, B. (1997). Simulations of lighting for an optimal defect detection by artificial vision, *IEEE/ASME International Conference on Advanced Intelligent Mechatronics* pp. 117–122.

Cowan, C. & Kovesi, P. (1988). Automatic sensor placement from vision task requirements, *IEEE Transaction on Pattern Analysis and Machine Intelligence* 10(3): 407–416.

Dunn, E.;Olague, G. (2005). Pareto optimal camera placement for automated visual inspection, *IEEE/RSJ International Conference on Intelligent Robots and Systems* pp. 3821–3826.

Eiben, A.E.;Smith, J. (2003). *Introduction to evolutionary computing*, Springer.

Forsyth, D. & Ponce, J. (2003). *Computer Vision: A Modern Approach*, Prentice Hall.

Guo, H.; Tao, T. (2007). Specular surface measurement by using a moving diffuse structured light source, *Proceedings of SPIE- The International Society for Optical Engineering* 6834(68343E).

Jahr, I. (2008). *Lighting in Machine Vision. Handbook of Machine Vision*, A. Hornberg, Wiley-VCH Verlag GmbH.

Kakikura, S. S. T. M. (1990). Automatic planning of light source placement for an active photometric stereo system, *IEEE International Workshop on Intelligent Robots and Systems* pp. 559–566.

Kutulakos, K. (2008). A theory of refractive and specular 3d shape by light-path triangulation, *International Journal of Computer Vision* 76: 13–29.

Malamas, E., Petrakis, E., Zervakis, M., Petit, L. & Legat, J.-D. (2003). A survey on industrial vision systems, applications and tools, *Image and Vision Computing* 21: 171–188.

Ng, H.-F. (2006). Automatic thresholding for defect detection, *Pattern Recognition Letters* 27: 1644– 1649.

Rosin, P. (2001). Unimodal thresholding, *Patter Recognition* 34(11): 2083–2096.

Russ, J. (2007). *The Image Processing Handbook*, fifth edition edn, Taylor and Francis.

Satorres Martínez, S. (2010). *Inspección automática de defectos en cristales de faros para automóviles mediante vision por computador*, PhD thesis, University of Jaén.

Satorres Martínez, S., Gómez Ortega, J., Gámez García, J. & Sánchez García, A. (2009a). An automatic procedure to code the inspection guideline for vehicle headlamp lenses, *IEEE International Conference on Mechatronic* .

Satorres Martínez, S., Gómez Ortega, J., Gámez García, J. & Sánchez García, A. (2009b). A dynamic lighting system for automated visual inspection of headlamp lenses, *14th IEEE International Conference on Emerging Techonologies and Factory Automation* .

Satorres Martínez, S., Gómez Ortega, J., Gámez García, J. & Sánchez García, A. (2009c). A machine vision system for defect characterization on transparent parts with non-plane surfaces, *Machine Vision with Applications (in review process)*.

Satorres Martínez, S., Gómez Ortega, J., Gámez García, J. & Sánchez García, A. (2009d). A sensor planning system for automated headlamp lens inspection, *Expert Systems with Applications* 36(5): 8768–8777.

Seulin, R., Merienne, F. & Gorria, P. (2001). Dynamic lighting system for specular surface inspection, *Machine Vision Applications in Industrial Inspection IX* 4301: 199–206.

Sheng,W., Xi, N., Song, M. & Chen, Y. (2003). Cad-guided sensor planning for dimensional inspection in automotive manufacturing, *IEEE/ASME Transaction on Mechatronics* 8(3): 372–380.

Sheng, W., Xi, N., Tan, J., Song, M. & Chen, Y. (2003). Minimum viewpoint planning for dimensional inspection of sheet metal parts, *Proceedings IEEE/ASME International Conference on Advanced Intelligent Mechatronics* pp. 1049–1054.

Tarabanis, K., Allen, P. & Tsai, R. (1995). A survey of sensor planning in computer vision, *IEEE Transaction on Robotics and Automation* 11(1): 86–104.

Tarabanis, K., Tsai, R. & Allen, P. (1995). The mvp sensor planning system for robotic vision tasks, *IEEE Transaction on Robotics and Automation* 11(1): 72–85.

Telljohann, A. (2008). *Introduction to Building a Machine Vision Inspection. Handbook of Machine Vision*, A. Hornberg, Wiley-VCH Verlag GmbH.

Wördenweber, B., Wallascheck, J., Boyce, P. & Hoffman, D. (2007). *Automotive Lighting and Human Vision*, Springer-Verlag Berlin Heidelberg.

Yi, S., Haralick, R. M. & Shapiro, L. G. (1990). Automatic sensor and light source positioning for machine vision, *Proc. 10th Int. Conf. Pattern Recognition* pp. 55–59.